Radiology

# Synovial Oxygenation at Photoacoustic Imaging to Assess Rheumatoid Arthritis Disease Activity

*Meng Yang, MD** • *Chenyang Zhao, MD** • *Ming Wang, MD* • *Qian Wang, MD* • *Rui Zhang, MD* • *Wei Bai, MD* • *Jian Liu, MD* • *Shangzhu Zhang, MD* • *Dong Xu, MD* • *Sirui Liu, MD* • *Xuelan Li, MD* • *Zhenhong Qi, MD* • *Fang Yang, PhD* • *Lei Zhu, PhD* • *Xujin He, MSc* • *Xinping Tian, MD* • *Xiaofeng Zeng, MD* • *Jianchu Li, MD* • *Yuxin Jiang, MD*

From the Departments of Ultrasound (M.Y., C.Z., M.W., R.Z., S.L., X.L., Z.Q., J. Li, Y.J.) and Rheumatology and Clinical Immunology (Q.W., W.B., S.Z., D.X., X.T., X.Z.), State Key Laboratory of Complex Severe and Rare Diseases, Peking Union Medical College Hospital, Chinese Academy of Medical Sciences and Peking Union Medical College, Shuaifuyuan No. 1, Dongcheng District, Beijing 100730, China; National Clinical Research Center for Dermatologic and Immunologic Diseases (NCRC-DID), Ministry of Science & Technology, and Key Laboratory of Rheumatology and Clinical Immunology, Ministry of Education, Beijing, China (Q.W., W.B., S.Z., D.X., X.T., X.Z.,); Department of Rheumatology, Aero Space Central Hospital, Beijing, China (J. Liu); and Shenzhen Mindray Bio-Medical Electronics Co, Ltd, Shenzhen, China (F.Y., L.Z., X.H.). Received September 8, 2021; revision requested October 26; revision received June 8, 2022; accepted July 15. **Address correspondence to** Y.J. (email: *jiangyx_pumch@163.com*).

Supported by the Beijing Natural Science Foundation (JQ18023), National Natural Science Foundation of China (61971447, 81301268, 81421004), Beijing Nova Program Interdisciplinary Cooperation Project (xxjc2018023), CAMS Innovation Fund for Medical Sciences (2020-I2M-C&T-B-035), Non-profit Central Research Institute Fund of Chinese Academy of Medical Sciences (2021-PT320-002), National Key Research and Development Program from the Ministry of Science and Technology of the People's Republic of China (2017YFE0104200), and International Science and Technology Cooperation Programme (2015DFA30440).

* M.Y. and C.Z. contributed equally to this work.

Conflicts of interest are listed at the end of this article.

**Radiology 2023; 306:220–228 • https://doi.org/10.1148/radiol.212257 • Content codes: MK US**

***Background:*** Synovial hypoxia is a hallmark of rheumatoid arthritis (RA). Photoacoustic (PA) imaging, based on the use of laser-generated US, can detect the oxygenation status of tissue in individuals with RA. However, large studies are lacking, with few investigating the correlation between oxygenation status and disease activity.

***Purpose:*** To measure synovial oxygenation status in participants with RA by using a multimodal PA US imaging system and to determine the correlation between PA imaging–measured oxygen saturation ($So_2$) and disease activity.

***Materials and Methods:*** In this prospective observational cohort study, multimodal PA US imaging examinations were performed on small joints of consecutive participants with RA, who were treated at two outpatient rheumatology clinics from 2019 to 2021, and healthy controls. The $So_2$ values of the synovium were measured with dual-wavelength PA imaging and classified into three categories—hyperoxia, intermediate oxygenation status, or hypoxia—based on the signal coloration and clustering analysis of the $So_2$ values. The correlations of oxygenation status with power Doppler US (PDUS) scoring and clinical disease activity index were evaluated with one-way analysis of variance and the Kruskal-Wallis test with Bonferroni correction.

***Results:*** A total of 118 participants with RA (median age, 55 years [IQR, 41–62 years]; 92 women) and 15 healthy control participants (median age, 37 years [IQR, 33–41 years]; 11 women) were included. The wrist synovium was categorized as hyperoxic in 36 participants with RA, of intermediate oxygenation status in 48 participants, and hypoxic in 34 participants. All control participants had hyperoxic synovial tissues. For participants with RA, hyperoxic synovium had more affluent Doppler US–depicted vasculature than those with hypoxia and intermediate oxygenation status (mean PDUS grade: hyperoxia, 2.7 ± 0.6 [SD]; intermediate, 1.3 ± 0.7; hypoxia, 1.1 ± 0.8; $P < .001$). Participants with intermediate status synovium had a lower clinical disease activity index than those with hypoxia (intermediate, 11.0 [IQR, 5.0–21.5] vs hypoxia, 26.0 [IQR, 18.0–39.0]; $P = .001$).

***Conclusion:*** Photoacoustic imaging–detected hypoxia in thickened synovium correlated with less vascularization and higher disease activity in participants with rheumatoid arthritis.

Clinical trial registration no. NCT04297475

© RSNA, 2022

*Online supplemental material is available for this article.*

Despite aggressive treatment, rheumatoid arthritis (RA) is a chronic autoimmune disease characterized by synovial inflammation. Recurring joint inflammation can further result in irreversible structural destruction and disability (1). US and MRI are sensitive methods used to assess arthritis (2). US has increasing importance in RA evaluation due to its low cost and improved resolution; however, previous studies have reported conflicting results, making its role debatable (3–7). Some studies have suggested that US could predict RA relapse following drug tapering (3), while some have denied the added value of US-driven disease management (6,7). Additionally, the correlation of US features with clinical disease activity has been relatively low (8,9). Therefore, to enhance the accuracy of US in assessing RA and further guiding treatment, it is advantageous to develop innovative tools that can provide additional information.

Tissue hypoxia, also known as low partial pressure of oxygen at the tissue level, is a hallmark of inflammatory diseases, including RA (10,11). Hypoxia triggers the

This copy is for personal use only. To order printed copies, contact *reprints@rsna.org*

## Abbreviations

CDAI = clinical disease activity index, DAS28 = 28-joint disease activity score, GSUS = gray-scale US, PA = photoacoustic, PDUS = power Doppler US, RA = rheumatoid arthritis, $So_2$ = oxygen saturation


## Summary

Thickened synovium with a hypoxic oxygenation status as measured with photoacoustic imaging was associated with fewer Doppler US signals and higher disease activity in study participants with rheumatoid arthritis.

## Key Results

- In this prospective study of 118 participants with rheumatoid arthritis (RA) and 15 control participants, the oxygen saturation values of the synovium measured with photoacoustic imaging were classified as hyperoxia, intermediate oxygenation status, or hypoxia.
- In participants with RA, hypoxia in thickened synovium had less local Doppler US–depicted vascularization than hyperoxic synovium (mean Doppler US grades, 2.7 vs 1.1; $P < .001$).
- Hypoxic joints had higher clinical disease activity than those with an intermediate oxygenation status (clinical disease activity index, 11.0 vs 26.0; $P = .001$).


activation and proliferation of abnormal immune cells and exacerbates the inflammatory response via complex signaling pathways, which also serve as a therapeutic target for RA (12–16). Hence, identifying hypoxia may aid in evaluating RA disease activity and tailoring treatment strategies. Previous studies have validated the existence of hypoxia in RA synovitis (17–20). However, detecting synovial hypoxia in vivo and revealing its role in RA remain a challenge.

Photoacoustic (PA) imaging, a revolutionary medical imaging technique based on laser-generated US, can help assess the oxygenation status in patients with RA (21). Notably, PA imaging can be integrated with US devices as dual-modal PA US imaging, facilitating its clinical promotion (22). Several studies have investigated PA imaging in patients with RA to evaluate arthritis (23–29). However, these studies have relatively small sample sizes, and few have investigated the correlation between PA imaging–measured oxygenation status and disease activity. A clinical study suggested that tissue hypoxia could be detected in patients with RA at PA imaging, which is associated with patient global activity and evaluator global activity (29). It is assumed that hypoxic synovium is correlated with US features and clinical disease activity. In this study, we performed PA imaging to assess the inflammatory activity in a larger sample of participants to further reveal the role of hypoxia in RA. We aimed to measure the oxygenation status of thickened synovium in study participants with RA by using a multimodal PA US imaging system, and to determine the correlation between oxygen saturation ($So_2$) levels measured with PA imaging and clinical scores.

## Materials and Methods

Mindray Bio-Medical Electronics helped develop the imaging system. The nonemployee authors had control of any included data. This is a prospective observational cohort study registered at ClinicalTrials.gov (registration no. NCT04297475). The institutional review board of our hospital authorized all operations conducted as part of this research (approval number: JS-1923), and all participants provided written informed consent.

### Participants

Five rheumatologists consecutively recruited eligible participants with RA at two outpatient rheumatology clinics from 2019 to 2021. Those older than 18 years who were diagnosed with RA according to the 2010 American College of Rheumatology and European League Against Rheumatism (now the European Alliance of Associations for Rheumatology) diagnostic criteria were enrolled (30). We also recruited healthy volunteers from the hospital staff as controls. A preliminary publication included 31 patients also included in this study (29). However, in this study, we enlarged the sample size and the imaging data were reanalyzed with different results.

### Multimodal PA US Imaging System and $So_2$ Mapping

The imaging system was developed on a commercial US machine (Mindray Bio-Medical Electronics) with a tunable optical parametric oscillator laser (InnoLas Laser), equipped with a handheld linear PA US L9–3 probe (imaging settings are detailed in Appendix E1 [online]). PA imaging was performed at two wavelengths, 750 nm and 830 nm, to measure $So_2$. The resultant PA imaging–measured $So_2$ (hereafter, PA-$So_2$) map was pseudocolored and superimposed onto the US image on the PA US system. Red and blue pixels represented high and low $So_2$ values, respectively. $So_2$ values were quantified automatically using an onboard algorithm (formulation and validation of PA-$So_2$ measurement is described in Appendix E1 and Figures E1–E3 [online]).

### Image Scoring and $So_2$ Subgrouping

Two radiologists (R.Z. and S.L., each with 5 years of experience in musculoskeletal US), who knew the name and age of participants but were blinded to their medical history, laboratory results, and clinical scores, performed multimodal PA US imaging on the dorsal second and third metacarpophalangeal joints, second and third proximal interphalangeal joints, second and fifth metatarsophalangeal joints, and wrists of the clinically dominant side longitudinally (31). Control participants underwent PA imaging of the wrist, and PA signals surrounding the normal synovium were analyzed. US was performed to evaluate synovitis before initiating PA imaging. Another two radiologists (C.Z. and M.W., each with 5 years of experience in musculoskeletal US), who were blinded to all participant information, reviewed the recorded images independently.

The two radiologists assessed US image scores based on European League Against Rheumatism–Outcomes Measures in Rheumatology US standards of synovial hypertrophy and Doppler US signals (Appendix E1 [online]) (32). They measured $So_2$ values three times for each joint. The PA-$So_2$ images had three types of pseudocolor combinations that included red-dominant signals, mixed-color signals, and blue-dominant signals. Eighty images of each type were selected by one radiologist for analysis, which were confirmed by the other radiologist subsequently. The $So_2$ values of the images ranged from 58% to 97%, which presented as three clusters on the

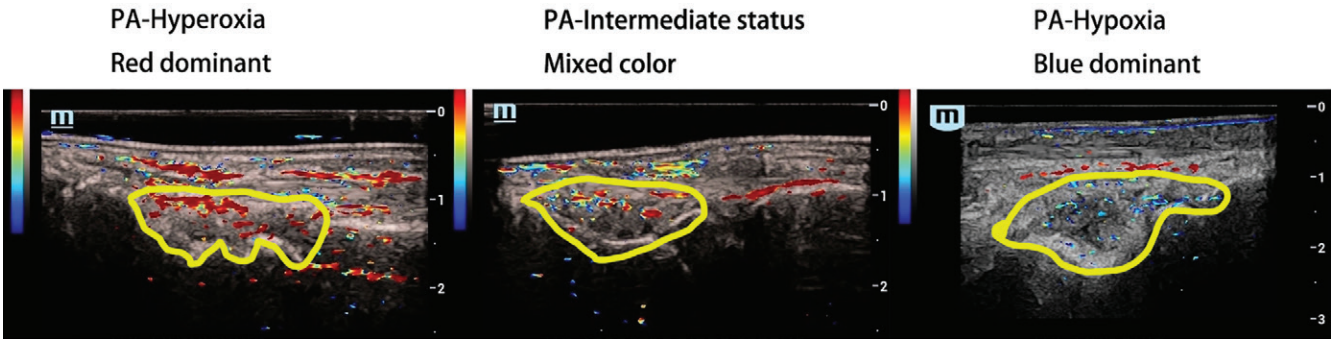


**Figure 1:** Oxygenation status groupings in thickened synovium. The oxygenation saturation ($So_2$) value is acquired by calculating the proportions of signal pixels in 750 nm and 830 nm photoacoustic (PA) images. Left: PA US image with $So_2$ mapping in pseudocolor shows red signals (circled) within the thickened synovium representing hyperoxia, with a relative $So_2$ value greater than 84%. Middle: PA US image with $So_2$ mapping in pseudocolor shows a mixture of red and blue signals (circled) representing intermediate oxygenation status, with a relative $So_2$ value of 70%–84%. Right: PA US image with $So_2$ mapping in pseudocolor shows blue signals (circled) within the thickened synovium representing hypoxia, with a relative $So_2$ value less than 70%. Imaging settings: luminous flux, less than 20 mJ/cm$^2$; fluctuation, less than 5%; imaging gain value, 45–55 dB; color bar, 40%–100%.

scatterplot. Hierarchical clustering analysis was performed to depict the scree diagram of distance coefficients, and the cluster number was determined as three according to the elbow rule. The cluster centers were then identified by k-means clustering as 89.64%, 78.48%, 65.73%, with ranges of greater than 84%, 70%–84%, and less than 70%, respectively (Appendix E1, Fig E4 [online]). On the basis of clustering analysis and types of pseudocolors, three types of oxygenation status were identified: hyperoxia, indicated by an $So_2$ level greater than 84% and predominantly red signals; intermediate oxygenation status, indicated by an $So_2$ level 70%–84% and a mixture of red and blue signals; and hypoxia, indicated by an $So_2$ level less than 70% and predominantly blue signals (Fig 1).

The images were reread by the two radiologists 1 month later. They reassessed any images with intraobserver or interobserver inconsistency. If consensus could not be reached, final results were determined by an expert (M.Y., with 15 years of experience in musculoskeletal US) blinded to all patient information.

### Clinical Evaluation

The clinical scores of participants with RA were assessed by two rheumatologists (Q.W. and S.Z., each with over 20 years of experience in rheumatology), including tender joint count, swollen joint count, visual analog scale for pain (0–100), patient global activity, evaluator global activity, 28-joint disease activity score (DAS28), simplified disease activity index, and clinical disease activity index (CDAI).

### Statistical Analysis

According to our pre-experiment, the mean PA $So_2$ values for wrist synovium of participants with RA and healthy controls were 78.0% ± 9.8 (SD) and 89.8% ± 2.0, respectively. A sample size of 118 participants with RA and 15 control participants gave a power of one at a one-sided significance of 2.5%.

Normally distributed data are expressed as means and SDs, nd were analyzed using the Student *t* test or one-way analysis of variance (ANOVA) for multiple group comparisons. The Student *t* test was performed for pairwise comparisons when the ANOVA test showed significant differences among the three groups. Nonnormal data are expressed as medians and IQRs. Nonnormal continuous data and categorical data were analyzed using the Mann-Whitney *U* test or Kruskal-Wallis H test for multiple groups comparisons. The Dunn pairwise test was performed when the Kruskal-Wallis test showed significant differences among the three groups. $P < .05$ was considered indicative of a statistically significant difference, and *P* values were adjusted with Bonferroni correction for post hoc multiple tests. The intraobserver and interobserver agreements of the two radiologists (C.Z. and M.W.) were evaluated using weighted κ values with 95% CIs. SPSS Statistics version 26.0 (IBM) was used for statistical analysis.

## Results

### Characteristics of Study Participants

A flow diagram of the study is illustrated in Figure 2. A total of 118 participants with RA and 15 healthy control participants were included and underwent multimodal PA US imaging and clinical assessment. The participants with RA included 26 men and 92 women (median age, 55 years [IQR, 41–62 years]). The control participants included four men and 11 women (median age, 37 years [IQR, 33–41 years]). Basic clinical information for participants with early- and late-stage RA is shown in Table 1.

### Intra- and Interobserver Variability

The two radiologists had excellent intraobserver agreement in gray-scale US (GSUS) (reader 1, κ = 0.92 [95% CI: 0.90, 0.94]; reader 2, κ = 0.91 [95% CI: 0.89, 0.92]), power Doppler US (PDUS) (reader 1, κ = 0.95 [95% CI: 0.94, 0.97]; reader 2, κ = 0.97 [95% CI: 0.95, 0.98]), and oxygenation status classification (reader 1, κ = 0.97 [95% CI: 0.95, 1.00]; reader 2, κ = 0.96 [95% CI: 0.92, 0.99]). They also reached excellent interobserver agreement on scoring of US images (GSUS, κ = 0.89 [95% CI: 0.87, 0.91]; PDUS, κ = 0.94 [95% CI: 0.93, 0.96]) and classifying oxygenation status (PA $So_2$, κ = 0.94 [95% CI: 0.91, 0.98]) (the reliability of PA -$So_2$ measurement is described in Appendix E1 and Figure E5 [online]).

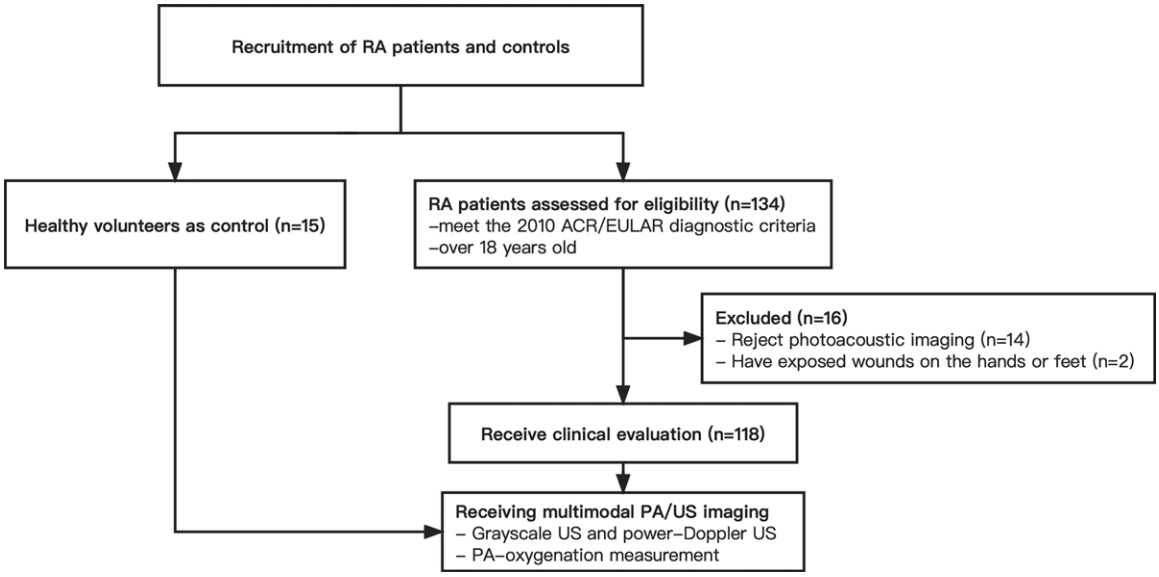


**Figure 2:** Study flow diagram. ACR/EULAR = American College of Rheumatology and European League Against Rheumatism, PA = photoacoustic, RA = rheumatoid arthritis.

### Comparison of PA-$So_2$ Values between Participants with RA and Controls

We compared the PA-$So_2$ values of wrist synovium of participants with RA with that of tissues surrounding the wrist synovium of controls. The PA-$So_2$ values of the wrist synovium of the participants with RA ranged from 58% to 95%. A total of 36 participants with RA were identified as having hyperoxia, 48 as having an intermediate oxygenation status, and 34 as having hypoxia in wrist synovium. The $So_2$ values of the wrist tissue of the control participants ranged from 88% to 96%, with all controls categorized as having hyperoxia. The participants with RA had more cases with reduced oxygenation than the volunteers (34 vs 0, $P < .001$).

### Correlations of PA-$So_2$ Values with PDUS Grades and Clinical Manifestations

We examined a total of 826 joints among the 118 participants by using the PA US system. As PA imaging signals could not be accurately observed for the joints with slightly thickened synovium or normal synovium (some GSUS grade 1 joints and all GSUS grade 0 joints), we measured PA-$So_2$ values of the synovium of 56 GSUS grade 1 joints, 145 GSUS grade 2 joints, and 98 GSUS grade 3 joints. The clinical manifestations and imaging characteristics of the seven types of joints that were examined are shown in Table 2.

Then we compared the PDUS grades of participants with RA who had identical GSUS scores and different oxygenation statuses (Table 3). There were 48 hyperoxic, 57 intermediate, and 40 hypoxic GSUS grade 2 joints and 26 hyperoxic, 33 intermediate, and 39 hypoxic GSUS grade 3 joints. The hyperoxia group had the highest mean PDUS grades for both GSUS grade 2 joints (hyperoxia, 1.6 ± 1.0; intermediate, 0.8 ± 0.6; hypoxia, 0.8 ± 0.6; $P < .001$) and GSUS grade 3 joints (hyperoxia, 2.7 ± 0.6; intermediate, 1.3 ± 0.7; hypoxia, 1.1 ± 0.8; $P < .001$). The results suggested that the thickened synovium with higher oxygenation levels had more affluent Doppler US–displayed vasculature than hypoxic and intermediate status synovium (Figs 3, 4). In GSUS grade 3 joints, hyperoxic joints had more tender joints than those in the intermediate oxygenation status group (hyperoxia, 18 of 49 [36.7%]; intermediate, 10 of 49 [20.4%]; $P = .009$).

### Correlations between PA-$So_2$ Values and Clinical Parameters

The PA-$So_2$ value of the joint that had the highest GSUS and PDUS grades was identified as the representative oxygenation status of each participant with RA. The participants with RA were subsequently divided into three oxygenation status groups: hyperoxia, intermediate oxygenation status, or hypoxia (Table 4).

Compared with the intermediate status group, the hypoxia group had higher median swollen (intermediate, 6.0 [IQR, 2.0–8.0]; hypoxia, 10.0 [IQR, 6.3–12.5]; $P = .01$) and tender joint counts (intermediate, 1.0 [IQR, 0.0–7.0]; hypoxia, 7.5 [IQR, 2.3–12.8]; $P = .003$). The hypoxia group also had higher median visual analog scale scores for pain (intermediate, 20.0 [IQR, 6.0–36.3]; hypoxia, 55.0 [IQR, 32.0–78.8]; $P < .001$), patient global activity scores (intermediate, 20.0 [IQR, 10.0–27.5]; hypoxia, 60.5 [IQR, 29.8–80.0]; $P < .001$), and evaluator global activity scores (intermediate, 23.5 [IQR, 15.0–30.0]; hypoxia, 40.0 [30.0–60.0]; $P = .003$). In addition, the hypoxia group had higher mean standard clinical scores, including the DAS28 with erythrocyte sedimentation rate (intermediate, 3.6 ± 1.5; hypoxia, 5.3 ± 1.8; $P < .001$) and DAS28 with C-reactive protein (intermediate, 3.2 ± 1.4; hypoxia, 4.7 ± 1.8; $P = .001$), and higher median simplified disease activity index (intermediate, 11.5 [IQR, 5.8–22.3]; hypoxia, 28.0 [IQR, 18.5–44.3]; $P < .001$) and CDAI (intermediate, 11.0 [IQR, 5.0–21.5]; hypoxia, 26.0 [IQR, 18.0–39.0]; $P = .001$) values. The hyperoxia group had a higher mean DAS28 with C-reactive protein (intermediate, 3.2 ± 1.4; hyperoxia,

**Table 1: Clinical Characteristics of Participants with RA according to Disease Duration**

| Characteristic | All Participants with RA (*n* = 118) | Early-Stage RA (<5 y) (*n* = 38) | Late-Stage RA (≥5 y) (*n* = 80) | *P* Value |
|---|---|---|---|---|
| Demographics | | | | |
| Age (y) | 55 (41–62) | 43 (30–59) | 57 (50–63) | <.006 |
| Sex* | | | | .86 |
| F | 92 (78) | 30 (79) | 62 (78) | |
| M | 26 (22) | 8 (21) | 18 (23) | |
| Height (cm) | 164.0 (158.0–168.0) | 166.0 (159.0–173.0) | 164.0 (158.0–167.0) | .14 |
| Weight (kg)† | 64.0 ± 10.2 | 64.7 ± 12.2 | 60.8 ± 9.3 | .24 |
| Onset time (y) | 7.0 (3.0–13.0) | 2.0 (1.8–3.0) | 12.0 (7.0–20.0) | <.001 |
| Cardiovascular or pulmonary complications* | 27 (23) | 7 (18) | 20 (25) | .43 |
| Laboratory tests | | | | |
| ESR (sec) | 18.0 (9.0–31.0) | 21.0 (9.0–34.5) | 17.0 (8.3–28.5) | .27 |
| CRP (mg/mL) | 3.0 (1.0–14.3) | 3.0 (1.0–12.0) | 3.0 (1.0–16.0) | .90 |
| Clinical manifestations | | | | |
| SJC | 7.0 (4.0–11.0) | 8.5 (6.8–12.0) | 6.0 (3.0–10.0) | .05 |
| TJC | 3.0 (0.0–8.8) | 7.0 (2.8–8.3) | 2.0 (0.0–8.8) | .11 |
| Disease evaluation scores | | | | |
| VAS for pain | 30.0 (15.0–50.0) | 30.0 (15.0–50.0) | 30.0 (10.5–52.3) | .76 |
| PGA | 29.0 (20.0–55.0) | 35.0 (20.0–52.5) | 25.0 (16.5–57.5) | .60 |
| EGA | 30.0 (15.0–50.0) | 30.0 (27.5–50.0) | 29.5 (15.0–50.0) | .19 |
| Standard clinical scores for disease activity | | | | |
| DAS28 ESR† | 4.4 ± 1.8 | 4.8 ± 1.3 | 4.1 ± 2.0 | .11 |
| DAS28 CRP† | 3.9 ± 1.7 | 4.3 ± 1.2 | 3.7 ± 1.9 | .14 |
| SDAI | 20.0 (10.0–31.0) | 24.0 (17.0–31.0) | 17.0 (7.5–31.8) | .11 |
| CDAI | 20.0 (10.0–29.3) | 23.0 (15.0–30.0) | 16.0 (7.5–28.8) | .14 |
| Activity status* | | | | .20 |
| Active | 74 (63) | 27 (71) | 47 (59) | |
| Remission | 44 (37) | 11 (29) | 33 (41) | |

Note.—Except where indicated, data are medians, with IQRs in parentheses. VAS for pain, PGA, and EGA are scored 0–100. DAS28 ESR or CRP is determined by the following equation: (0.56 × square (TJC)) + (0.28 × square (SJC)) + (0.7 × natural logarithm (ESR/CRP)) + (0.014 × PGA). SDAI is defined as SJC plus TJC plus EGA/10 plus CRP, and CDAI is defined as SJC plus TJC plus PGA/10 plus EGA/10. Remission is defined by a DAS28 ESR or DAS28 CRP score less than 2.8. CDAI = clinical disease activity index, CRP = C-reactive protein, DAS28 = 28-joint disease activity score, EGA = evaluator global assessment, ESR = erythrocyte sedimentation rate, PGA = patient global assessment, RA = rheumatoid arthritis, SDAI = simplified disease activity index, SJC = swollen joint count, TJC = tender joint count, VAS = visual analog scale.

* Data are numbers of participants, with percentages in parentheses.

† Data are means ± SDs.

**Table 2: Imaging Characteristics and Clinical Manifestations of Specific Joints**

| Joint | No. of Joints | Swollen Joint Count | Tender Joint Count | GSUS Grade ≥1 | PDUS Grade ≥1 | PA-$So_2$ Identified | Hyperoxia | Intermediate | Hypoxia |
|---|---|---|---|---|---|---|---|---|---|
| MCP2 | 118 | 57/118 (48) | 27/118 (22.8) | 98/118 (83.1) | 48/118 (40.7) | 68/118 (57.6) | 23/68 (33.8) | 30/68 (44.1) | 15/68 (22.1) |
| MCP3 | 118 | 45/118 (38.1) | 22/118 (18.6) | 72/118 (61.0) | 29/118 (24.6) | 43/118 (36.4) | 14/43 (32.5) | 16/43 (37.2) | 12/43 (27.9) |
| PIP2 | 118 | 41/118 (34.7) | 20/118 (16.9) | 10/118 (8.5) | 9/118 (7.7) | 12/118 (10.2) | 6/12 (50.0) | 2/12 (16.7) | 4/12 (33.3) |
| PIP3 | 118 | 53/118 (44.9) | 22/118 (18.6) | 30/118 (25.4) | 8/118 (6.8) | 12/118 (10.2) | 5/12 (41.7) | 3/12 (25.0) | 4/12 (33.3) |
| MTP2 | 118 | 8/118 (6.8) | 5/118 (4.2) | 84/118 (71.2) | 14/118 (11.9) | 39/118 (33.1) | 12/39 (30.8) | 16/39 (41.0) | 11/39 (28.2) |
| MTP5 | 118 | 6/118 (5.1) | 4/118 (3.4) | 29/118 (24.5) | 3/118 (2.5) | 8/118 (6.8) | 0 (0) | 4/8 (50.0) | 4/8 (50.0) |
| Wrist | 118 | 68/118 (57.6) | 49/118 (41.5) | 118/118 (100) | 96/118 (81.3) | 118/118 (100) | 36/118 (30.5) | 48/118 (40.7) | 34/118 (28.8) |
| All | 826 | 278/826 (33.7) | 110/826 (13.3) | 441/826 (53.4) | 207/826 (25.1) | 299/826 (36.2) | 96/299 (32.1) | 119/299 (39.8) | 84/299 (28.1) |

Note.—Data are numbers of joints, with percentages in parentheses. PA-$So_2$ is the PA imaging–measured oxygen saturation level. Hyperoxia, intermediate oxygenation status, and hypoxia were determined according to PA-$So_2$. See Appendix E1 (online) for GSUS and PDUS grade definitions according to the imaging scoring methods used. GSUS = gray-scale US, MCP2 = second metacarpophalangeal joint, MCP3 = third metacarpophalangeal joint, MTP2 = second metatarsophalangeal joint, MTP5 = fifth metatarsophalangeal joint, PA = photoacoustic, PDUS = power Doppler US, PIP2 = second proximal interphalangeal joint, PIP3 = third proximal interphalangeal joint.

**Table 3: PDUS Grades and Clinical Manifestations of GSUS Grade 2 and GSUS Grade 3 Joints**

| Parameter | Total | Hyperoxia Group | Intermediate Group | Hypoxia Group | *P* Value | *P* Value* | *P* Value† | *P* Value‡ |
|---|---|---|---|---|---|---|---|---|
| GSUS grade 2 | | | | | | | | |
| No. | 145 | 48/145 (33.1) | 57/145 (39.3) | 40/145 (27.6) | | | | |
| PDUS grade | | | | | | | | |
| 0 | 35 | 6/35 (17.1) | 17/35 (48.6) | 12/35 (34.3) | .08 | … | … | … |
| 1 | 80 | 20/80 (25.0) | 35/80 (43.8) | 25/80 (31.3) | .06 | … | … | … |
| 2 | 16 | 8/16 (50.0) | 5/16 (31.3) | 3/16 (18.8) | .32 | … | … | … |
| 3 | 14 | 14/14 (100.0) | 0 (0.0) | 0 (0.0) | <.001 | <.001 | <.001 | >.99 |
| mean§ | 1.1 ± 0.9 | 1.6 ± 1.0 | 0.80 ± 0.59 | 0.78 ± 0.58 | <.001 | <.001 | <.001 | >.99 |
| Swollen joint count | 70 | 18/70 (25.7) | 29/70 (41.4) | 23/70 (32.9) | .16 | … | … | … |
| Tender joint count | 45 | 19/45 (42.2) | 12/45 (26.7) | 14/45 (31.1) | .12 | … | … | … |
| GSUS grade 3 | | | | | | | | |
| No. | 98 | 26/98 (26.5) | 33/98 (33.7) | 39/98 (39.8) | | | | |
| PDUS grade | | | | | | | | |
| 0 | 13 | 0 (0) | 4/13 (30.7) | 9/13 (69.2) | .03 | .53 | .02 | .52 |
| 1 | 35 | 2/35 (5.7) | 16/35 (45.7) | 17/35 (48.6) | .002 | .004 | .01 | >.99 |
| 2 | 29 | 3/29 (10.4) | 13/29 (44.8) | 13/29 (44.8) | .05 | … | … | … |
| 3 | 21 | 21/21 (100.0) | 0 (0.0) | 0 (0.0) | <.001 | <.001 | <.001 | >.99 |
| mean§ | 1.6 ± 1.0 | 2.7 ± 0.6 | 1.3 ± 0.7 | 1.1 ± 0.8 | <.001 | <.001 | <.001 | >.99 |
| Swollen joint count | 74 | 24/74 (32.4) | 23/74 (31.1) | 27/74 (36.5) | .07 | … | … | … |
| Tender joint count | 49 | 18/49 (36.7) | 10/49 (20.4) | 21/49 (42.9) | .01 | .009 | .68 | .14 |

Note.—Except where indicated, data are numbers of joints, with percentages in parentheses. Hyperoxia, intermediate oxygenation status, and hypoxia were determined according to photoacoustic imaging–measured oxygen saturation level. GSUS grade 2 indicates moderate synovitis with synovial hypertrophy with or without flow extending beyond the joint line and the convex upper surface or hypertrophy extending beyond the joint line but with a flat upper surface. GSUS grade 3 indicates severe synovitis with thickened synovium extending beyond the joint line and up to the level of the horizontal line connecting bone surfaces. *P* values were adjusted by using Bonferroni correction for multiple tests. Multiple comparisons were not performed when the overall tests did not show significant differences across samples. GSUS = gray-scale US, PDUS = power Doppler US.

* Comparison of the hyperoxia and intermediate oxygenation groups.

† Comparison of the hyperoxia and hypoxia groups.

‡ Comparison of the hypoxia and intermediate oxygenation groups.

§ Data are means ± SDs.

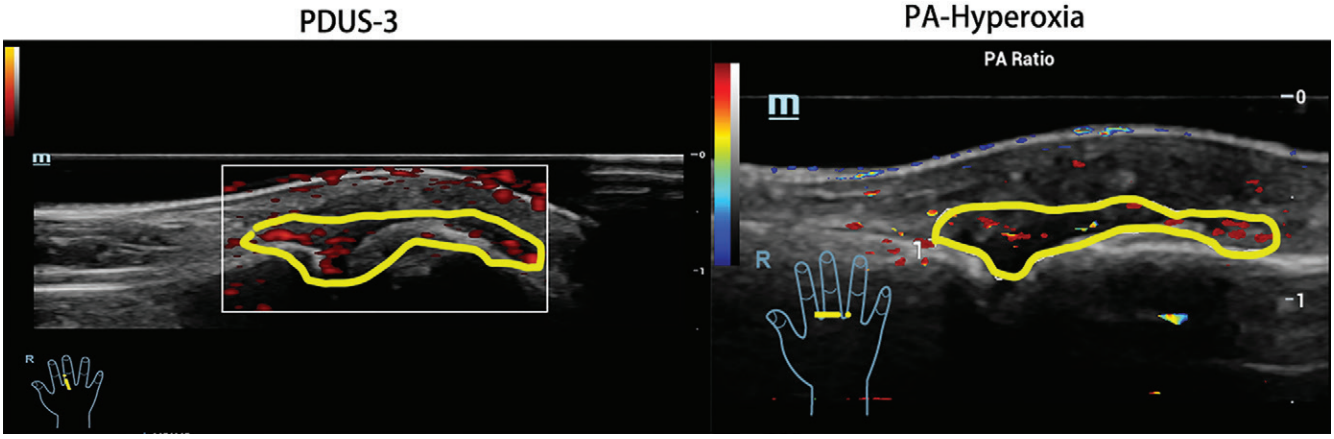


**Figure 3:** Example of power Doppler US (PDUS)–depicted hypervascularity and photoacoustic (PA) imaging–detected hyperoxia. The longitudinal section of (left) PDUS and (right) photoacoustic oxygenation saturation ($So_2$) images in the right (R) third metacarpophalangeal joint of a 36-year-old woman, who had lived with rheumatoid arthritis for 4 years and experienced joint swelling and pain, show the joint had a PDUS grade 3 (abundant signals in more than half of the synovium; circled, left) and the PA-$So_2$ mapping was red-dominant (circled, right), identified as hyperoxia. Imaging settings: luminous flux, less than 20 mJ/cm$^2$; fluctuation, less than 5%; imaging gain value, 45–55 dB; color bar, 40%–100%. For image scoring methods, see Appendix E1 (online).

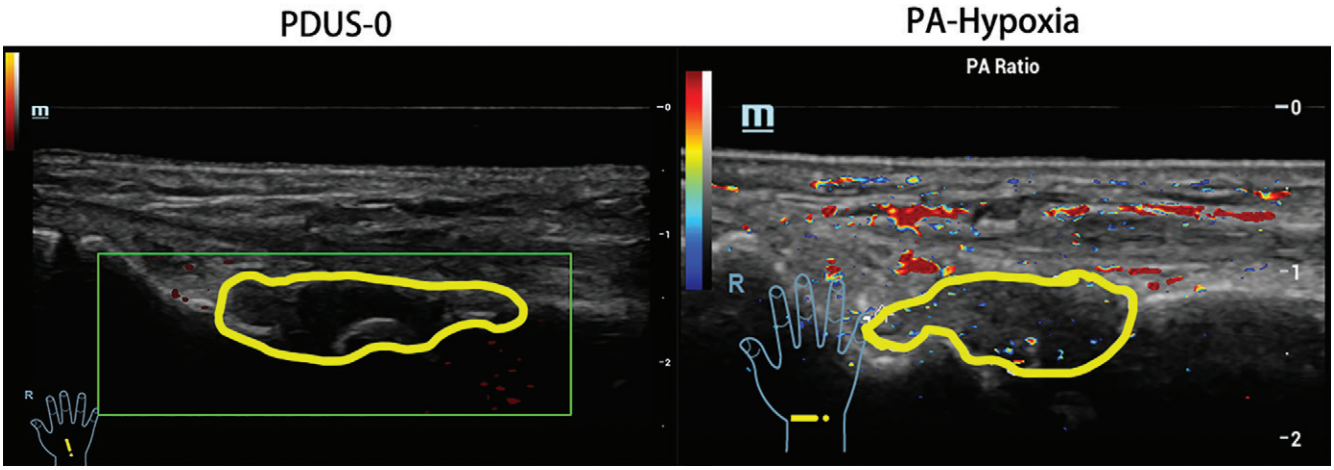


**Figure 4:** Example of power Doppler US (PDUS)–depicted hypovascularity and photoacoustic (PA) imaging–detected hypoxia. The longitudinal section of (left) PDUS and (right) PA oxygenation saturation ($So_2$) images in the right (R) wrist of a 65-year-old woman, who had lived with rheumatoid arthritis for 12 years and experienced recurrent wrist swelling and pain, show the wrist had a PDUS grade 0 (no signal; circled, left) and the wrist synovium was hypoxic based on the blue-dominant signals (circled, right) of PA-$So_2$ mapping. Imaging settings: luminous flux, less than 20 mJ/cm$^2$; fluctuation, less than 5%; imaging gain value, 45–55 dB; color bar, 40%–100%. For image scoring methods, see Appendix E1 (online).

**Table 4: Clinical Indexes of Participants with Different Oxygenation Statuses as Determined with Photoacoustic Imaging**

| Parameter | Hyperoxia Group ($n$ = 36) | Intermediate Group ($n$ = 51) | Hypoxia Group ($n$ = 31) | $P$ Value | $P$ Value* | $P$ Value† | $P$ Value‡ |
|---|---|---|---|---|---|---|---|
| Age (y) | 51 (38–58) | 54 (35–62) | 57 (53–66) | .01 | >.99 | .01 | .046 |
| Onset time (y) | 9.0 (3.0–12.0) | 6.0 (3.0–8.0) | 10.0 (4.5–21.0) | .15 | … | … | … |
| Cardiovascular or pulmonary complications§ | 6/27 (22) | 6/27 (22) | 15/27 (56) | <.001 | >.99 | .006 | <.001 |
| ESR (sec) | 20.0 (7.5–35.0) | 12.5 (7.8–23.5) | 24.0 (13.3–46.3) | .08 | … | … | … |
| CRP (mg/mL) | 6.0 (2.0–17.5) | 2.0 (1.0–6.3) | 9.0 (2.0–31.0) | .01 | .06 | >.99 | .03 |
| SJC | 10.0 (6.0–14.5) | 6.0 (2.0–8.0) | 10.0 (6.3–12.5) | .003 | .01 | >.99 | .01 |
| TJC | 3.0 (0.5–8.5) | 1.0 (0.0–7.0) | 7.5 (2.3–12.8) | .004 | .45 | .30 | .003 |
| VAS pain score | 30.0 (15.0–55.0) | 20.0 (6.0–36.3) | 55.0 (32.0–78.8) | <.001 | .19 | .11 | <.001 |
| PGA | 35.0 (20.0–50.0) | 20.0 (10.0–27.5) | 60.5 (29.8–80.0) | <.001 | .08 | .24 | <.001 |
| EGA | 30.0 (20.0–52.5) | 23.5 (15.0–30.0) | 40.0 (30.0–60.0) | .002 | .25 | .38 | .003 |
| DAS28 ESR‖ | 4.5 ± 1.9 | 3.6 ± 1.5 | 5.3 ± 1.8 | <.001 | .11 | .29 | <.001 |
| DAS28 CRP‖ | 4.2 ± 1.6 | 3.2 ± 1.4 | 4.7 ± 1.8 | <.001 | .04 | .65 | .001 |
| SDAI | 23.0 (14.5–32.0) | 11.5 (5.8–22.3) | 28.0 (18.5–44.3) | <.001 | .03 | .87 | <.001 |
| CDAI | 23.0 (13.0–30.5) | 11.0 (5.0–21.5) | 26.0 (18.0–39.0) | <.001 | .045 | .80 | .001 |
| Remission§ | 8/44 (18) | 31/44 (70) | 5/44 (11) | <.001 | .001 | >.99 | <.001 |

Note.—Except where indicated, data are medians, with IQRs in parentheses. VAS for pain, PGA, and EGA are scored 0–100. DAS28 ESR or CRP is determined by the following equation: (0.56 × square (TJC)) + (0.28 × square (SJC)) + (0.7 × natural logarithm (ESR/CRP)) + (0.014 × PGA). SDAI is defined as SJC plus TJC plus EGA/10 plus CRP, and CDAI is defined as SJC plus TJC plus PGA/10 plus EGA/10. Remission is defined by a DAS28 ESR or DAS28 CRP score less than 2.8. $P$ values were adjusted by using Bonferroni correction for multiple tests. Multiple comparisons were not performed when the overall tests did not show significant differences across samples. CDAI = clinical disease activity index, CRP = C-reactive protein, DAS28 = 28-joint disease activity score, EGA = evaluator global assessment, ESR = erythrocyte sedimentation rate, PGA = patient global assessment, SDAI = simplified disease activity index, SJC = swollen joint count, TJC = tender joint count, VAS = visual analog scale.

* Comparison of the hyperoxia and intermediate oxygenation groups.

† Comparison of the hyperoxia and hypoxia groups.

‡ Comparison of the hypoxia and intermediate oxygenation groups.

§ Data are numbers of participants, with percentages in parentheses.

‖ Data are means ± SDs.

4.2 ± 1.6; $P$ = .04) and higher median simplified disease activity index (intermediate, 11.5 [IQR, 5.8–22.3]; hyperoxia, 23.0 [IQR, 14.5–32.0]; $P$ = .03) and CDAI (intermediate, 11.0 [IQR, 5.0–21.5]; hyperoxia, 23.0 [IQR, 13.0–30.5]; $P$ = .045) values than the intermediate group. In the intermediate status group, 31 of 44 (70%) participants had clinical remission, more than that of the hyperoxia (eight of 44 [18%], $P$ = .001) and hypoxia (five of 44 [11%], $P$ < .001) groups. In the hypoxia group, 15 of 27 (56%) participants also had cardiovascular or pulmonary complications, which is more than that of the hyperoxia (six of 27 [22%], $P$ = .006) and intermediate status (six of 27 [12%], $P$ < .001) groups.

Among those joints with thickened synovium identified as hypoxic at PA imaging, a total of 39 GSUS grade 3 joints in 22 participants with RA had less vascularity, including nine PDUS grade 0, 17 PDUS grade 1, and 13 PDUS grade 2 joints. These 22 participants with RA had higher clinical disease activity, including the DAS28 with erythrocyte sedimentation rate (mean score: hypoxia group, 5.7 ± 1.6; all participants, 4.4 ± 1.8; $P$ = .003) and CDAI (median value: hypoxia group, 28.5 [IQR, 9.0–64.0]; all participants, 20.0 [IQR, 10.0–29.3]; $P$ = .004), than that of all participants with RA despite their lower PDUS grades, indicating that thickened synovium with less Doppler US vascularity and PA imaging–detected hypoxia might be associated with relatively high RA disease activity.

## Discussion

The presence of tissue hypoxia in patients with rheumatoid arthritis (RA) has been revealed by previous studies (17–20). However, a noninvasive method for measuring synovial oxygenation is still lacking, and there is limited information about synovial hypoxia in patients with RA. In this study, we used photoacoustic imaging, a new imaging technique based on laser-generated US, to noninvasively assess synovial oxygenation in study participants with RA and explore the relationship of oxygenation status with clinical evaluations. A total of 34 of 118 participants with RA were classified as having hypoxia in wrist synovium, while the 15 control participants were all identified as having hyperoxia. The wrist tissue of participants with RA had more cases with reduced oxygenation than that of the volunteers (34 vs 0, $P$ < .001). The synovium with lower oxygenation levels had less Doppler US–depicted vasculature than hyperoxic synovium (mean power Doppler US grade: hyperoxia, 2.7 ± 0.6; intermediate, 1.3 ± 0.7; and hypoxia, 1.1 ± 0.8; $P$ < .001). Participants with RA with hypoxic synovium had higher mean disease activity scores than those with intermediate oxygenation, including the 28-joint disease activity score with erythrocyte sedimentation rate (intermediate, 3.6 ± 1.5; hypoxia, 5.3 ± 1.8; $P$ < .001) and clinical disease activity index (intermediate, 11.0 [IQR, 5.0–21.5]; hypoxia, 26.0 [IQR, 18.0–39.0]; $P$ = .001).

Researchers have previously used PA imaging to evaluate patients with RA (23–28), but PA imaging oxygenation measurement for patients with RA still requires further investigation. Based on our preliminary clinical study (29), we expanded the sample size to draw a more robust conclusion regarding the correlation between tissue hypoxia and joint inflammation in the current study. Similar to previous studies on synovial hypoxia, we detected tissue hypoxia within the thickened synovium in participants with RA (19,33). An interesting finding of our study was that thickened synovium with abundant Doppler US signals tended to be identified as tissue hyperoxia, while those with less blood flow were found to have lower oxygenation levels. A similar phenomenon was also reported by Liu et al (34), who performed PA imaging in the knee joints of rats with posttraumatic osteoarthritis and found that both Doppler US blood flow and PA imaging oxygenation of the knee synovium were significantly decreased after surgery. This might be explained by the fact that synovial vessels that could be depicted by Doppler US were functional vascular structures with relatively high velocity, which could deliver oxygen to local tissues and increase oxygenation levels. For the thickened synovium without abundant synovial vessels, a lower oxygenation level could be detected.

We found that participants with hypoxic synovium had higher disease activity than those with intermediate oxygenation status synovium, which was in accordance with knowledge about the role of hypoxia in inflammation. Participants with hyperoxic synovium also had higher clinical scores than those with intermediate status synovium. Therefore, we inferred that patients with hyperoxic synovium might be in the active phase of inflammation, with increasing metabolism in local tissues in which oxygen supply is subsequently enhanced through the increased synovial vessels. In contrast, for the thickened synovium without abundant synovial vessels, a lower oxygenation level was detected due to insufficient oxygen supply. Moreover, in this study, we observed that joints with less vascularity and hypoxic synovium tended to represent higher disease activity. Conventionally, radiologists consider RA joints with more Doppler US signals to potentially represent higher inflammation activity. Based on our findings, we suggest that patients with low Doppler US scores but with the presence of synovial hypoxia might still be in a high disease activity state. Hence, PA imaging–detected synovial hypoxia could be a useful indicator for complementing US in RA evaluation.

Our study has several limitations. First, we lacked a reference standard for tissue oxygenation measured by established invasive methods. MRI is an essential imaging modality for RA and can be used as the reference standard to investigate other imaging modalities (35,36); however, we did not perform MRI for the participants in this study. In addition, the frequency of the PA US probe was relatively low. Moreover, the study controls were hospital employees, who were nonprobability samples and not representative of the general population, and the control group had significantly fewer participants than the RA group. Therefore, selection bias existed in this study.

To conclude, in this study, we performed multimodal photoacoustic (PA) US imaging and assessed the tissue oxygenation status of the thickened synovium in patients with rheumatoid arthritis (RA). PA imaging–detected hypoxia in thickened synovium was associated with less local vascularization and higher RA disease activity. To further explore the clinical utility of PA imaging for detection of hypoxia in RA management, PA imaging follow-up in a well-managed cohort of patients with RA is needed. MRI should

be added as an important contrast for PA imaging in future studies. In addition, we plan to improve the frequency and resolution of the PA US probe in subsequent investigations.

**Acknowledgment:** We thank Professor Xu Tao, PhD, for his help in the statistical analysis of the study.

**Author contributions:** Guarantors of integrity of entire study, **M.Y., C.Z., J. Liu, S.Z., Z.Q., F.Y., L.Z., X.H., X.Z., J. Li, X.J.**; study concepts/study design or data acquisition or data analysis/interpretation, all authors; manuscript drafting or manuscript revision for important intellectual content, all authors; approval of final version of submitted manuscript, all authors; agrees to ensure any questions related to the work are appropriately resolved, all authors; literature research, **C.Z., Q.W., J. Liu, D.X., X.T.**; clinical studies, all authors; experimental studies, **W.B., J. Liu, X.T.**; statistical analysis, **C.Z., R.Z., W.B., S.L., X.L., X.T.**; and manuscript editing, **M.Y., C.Z., Q.W., D.X., X.T.**

**Data sharing:** Data generated or analyzed during the study are available from the corresponding author by request.

**Disclosures of conflicts of interest: M.Y.** No relevant relationships. **C.Z.** No relevant relationships. **M.W.** No relevant relationships. **Q.W.** No relevant relationships. **R.Z.** No relevant relationships. **W.B.** No relevant relationships. **J. Liu** No relevant relationships. **S.Z.** No relevant relationships. **D.X.** No relevant relationships. **S.L.** **X.L.** No relevant relationships. **Z.Q.** No relevant relationships. **F.Y.** No relevant relationships. **L.Z.** No relevant relationships. **X.H.** No relevant relationships. **X.T.** No relevant relationships. **X.Z.** No relevant relationships. **J. Li** No relevant relationships. **Y.J.** No relevant relationships.

## References


1. Matcham F, Scott IC, Rayner L, et al. The impact of rheumatoid arthritis on quality-of-life assessed using the SF-36: a systematic review and meta-analysis. Semin Arthritis Rheum 2014;44(2):123–130.
2. Colebatch AN, Edwards CJ, Østergaard M, et al. EULAR recommendations for the use of imaging of the joints in the clinical management of rheumatoid arthritis. Ann Rheum Dis 2013;72(6):804–814.
3. Naredo E, Valor L, De la Torre I, et al. Predictive value of Doppler ultrasound-detected synovitis in relation to failed tapering of biologic therapy in patients with rheumatoid arthritis. Rheumatology (Oxford) 2015;54(8):1408–1414.
4. Iwamoto T, Ikeda K, Hosokawa J, et al. Prediction of relapse after discontinuation of biologic agents by ultrasonographic assessment in patients with rheumatoid arthritis in clinical remission: high predictive values of total gray-scale and power Doppler scores that represent residual synovial inflammation before discontinuation. Arthritis Care Res (Hoboken) 2014;66(10):1576–1581.
5. D'Agostino MA, Wakefield RJ, Berner-Hammer H, et al. Value of ultrasonography as a marker of early response to abatacept in patients with rheumatoid arthritis and an inadequate response to methotrexate: results from the APPRAISE study. Ann Rheum Dis 2016;75(10):1763–1769.
6. Haavardsholm EA, Aga AB, Olsen IC, et al. Ultrasound in management of rheumatoid arthritis: ARCTIC randomised controlled strategy trial. BMJ 2016;354:i4205.
7. Dale J, Stirling A, Zhang R, et al. Targeting ultrasound remission in early rheumatoid arthritis: the results of the TaSER study, a randomised clinical trial. Ann Rheum Dis 2016;75(6):1043–1050.
8. Tan YK, Li H, Allen JC Jr, Thumboo J. Ultrasound power Doppler and gray scale joint inflammation: What they reveal in rheumatoid arthritis. Int J Rheum Dis 2019;22(9):1719–1723.
9. Zufferey P, Courvoisier DS, Nissen MJ, et al. Discordances between clinical and ultrasound measurements of disease activity among RA patients followed in real life. Joint Bone Spine 2020;87(1):57–62.
10. McGarry T, Biniecka M, Veale DJ, Fearon U. Hypoxia, oxidative stress and inflammation. Free Radic Biol Med 2018;125:15–24.
11. Quiñonez-Flores CM, González-Chávez SA, Pacheco-Tena C. Hypoxia and its implications in rheumatoid arthritis. J Biomed Sci 2016;23(1):62.
12. Ahn JK, Koh EM, Cha HS, et al. Role of hypoxia-inducible factor-1alpha in hypoxia-induced expressions of IL-8, MMP-1 and MMP-3 in rheumatoid fibroblast-like synoviocytes. Rheumatology (Oxford) 2008;47(6):834–839.
13. Biniecka M, Fox E, Gao W, et al. Hypoxia induces mitochondrial mutagenesis and dysfunction in inflammatory arthritis. Arthritis Rheum 2011;63(8):2172–2182.
14. Gao W, McCormick J, Connolly M, Balogh E, Veale DJ, Fearon U. Hypoxia and STAT3 signalling interactions regulate pro-inflammatory pathways in rheumatoid arthritis. Ann Rheum Dis 2015;74(6):1275–1283.
15. Fan SS, Zong M, Zhang H, Lu Y, Lu TB, Fan LY. Decreased expression of alpha-enolase inhibits the proliferation of hypoxia-induced rheumatoid arthritis fibroblasts-like synoviocytes. Mod Rheumatol 2015;25(5):701–707.
16. Kennedy A, Ng CT, Chang TC, et al. Tumor necrosis factor blocking therapy alters joint inflammation and hypoxia. Arthritis Rheum 2011;63(4):923–932.
17. Lund-Olesen K. Oxygen tension in synovial fluids. Arthritis Rheum 1970;13(6):769–776.
18. Ng CT, Biniecka M, Kennedy A, et al. Synovial tissue hypoxia and inflammation in vivo. Ann Rheum Dis 2010;69(7):1389–1395.
19. Richman AI, Su EY, Ho G Jr. Reciprocal relationship of synovial fluid volume and oxygen tension. Arthritis Rheum 1981;24(5):701–705.
20. Sivakumar B, Akhavani MA, Winlove CP, Taylor PC, Paleolog EM, Kang N. Synovial hypoxia as a cause of tendon rupture in rheumatoid arthritis. J Hand Surg Am 2008;33(1):49–58.
21. Treuhaft PS, McCarty DJ. Synovial fluid pH, lactate, oxygen and carbon dioxide partial pressure in various joint diseases. Arthritis Rheum 1971;14(4):475–484.
22. Steinberg I, Huland DM, Vermesh O, Frostig HE, Tummers WS, Gambhir SS. Photoacoustic clinical imaging. Photoacoustics 2019;14:77–98.
23. Kuniyil Ajith Singh M, Xia W. Portable and Affordable Light Source-Based Photoacoustic Tomography. Sensors (Basel) 2020;20(21):E6173.
24. van den Berg PJ, Daoudi K, Bernelot Moens HJ, Steenbergen W. Feasibility of photoacoustic/ultrasound imaging of synovitis in finger joints using a point-of-care system. Photoacoustics 2017;8:8–14.
25. Jo J, Xu G, Cao M, et al. A Functional Study of Human Inflammatory Arthritis Using Photoacoustic Imaging. Sci Rep 2017;7(1):15026.
26. Jo J, Tian C, Xu G, et al. Photoacoustic tomography for human musculoskeletal imaging and inflammatory arthritis detection. Photoacoustics 2018;12:82–89.
27. Jo J, Xu G, Zhu Y, et al. Detecting joint inflammation by an LED-based photoacoustic imaging system: a feasibility study. J Biomed Opt 2018;23(11):1–4.
28. Nishiyama M, Namita T, Kondo K, Yamakawa M, Shiina T. Ring-array photoacoustic tomography for imaging human finger vasculature. J Biomed Opt 2019;24(9):1–12.
29. Guo H, Wang Q, Qi W, Sun X, Ke B, Xi L. Assessing the development and treatment of rheumatoid arthritis using multiparametric photoacoustic and ultrasound imaging. J Biophotonics 2019;12(11):e201900127.
30. Zhao C, Wang Q, Tao X, et al. Multimodal photoacoustic/ultrasonic imaging system: a promising imaging method for the evaluation of disease activity in rheumatoid arthritis. Eur Radiol 2021;31(5):3542–3552.
31. Aletaha D, Neogi T, Silman AJ, et al. 2010 Rheumatoid arthritis classification criteria: an American College of Rheumatology/European League Against Rheumatism collaborative initiative. Arthritis Rheum 2010;62(9):2569–2581.
32. Backhaus M, Ohrndorf S, Kellner H, et al. Evaluation of a novel 7-joint ultrasound score in daily rheumatologic practice: a pilot project. Arthritis Rheum 2009;61(9):1194–1201.
33. D'Agostino MA, Terslev L, Aegerter P, et al. Scoring ultrasound synovitis in rheumatoid arthritis: a EULAR-OMERACT ultrasound taskforce-Part 1: definition and development of a standardised, consensus-based scoring system. RMD Open 2017;3(1):e000428.
34. Liu Z, Au M, Wang X, et al. Photoacoustic imaging of synovial tissue hypoxia in experimental post-traumatic osteoarthritis. Prog Biophys Mol Biol 2019;148:12–20.
35. Takase-Minegishi K, Horita N, Kobayashi K, et al. Diagnostic test accuracy of ultrasound for synovitis in rheumatoid arthritis: systematic review and meta-analysis. Rheumatology (Oxford) 2018;57(1):49–58.
36. Ohrndorf S, Boer AC, Boeters DM, et al. Do musculoskeletal ultrasound and magnetic resonance imaging identify synovitis and tenosynovitis at the same joints and tendons? A comparative study in early inflammatory arthritis and clinically suspect arthralgia. Arthritis Res Ther 2019;21(1):59.